

Numerical simulation of single phase flow in a flotation machine

Ireneusz Szczygieł, Adam Fic, Andrzej Sachajdak, Marek Rojczyk,
Zbigniew Buliński

*Institute of Thermal Technology, Silesian University of Technology
Konarskiego 22, 44-100 Gliwice, Poland*

*e-mail: ireneusz.szczygiel@polsl.pl, adam.fic@polsl.pl, andrzej.sachajdak@polsl.pl,
marek.rojczyk@polsl.pl, zbigniew.bulinski@polsl.pl*

Adam Mańka

*Institute of Non-Ferrous Metals
Sowińskiego 5, 44-100 Gliwice, Poland
e-mail: adamm@imm.gliwice.pl*

In the paper, the numerical model of the flow phenomena in the flotation machine is presented. The process of flotation consists of a number of phenomena which provide serious numerical difficulties. One can enumerate rotation, two phase flow, foam formation etc. To the knowledge of authors there is no complete numerical model available for the flotation machine. The long-term task of the project is to create a complete model of the machine. Such a model would be very helpful in the process of construction and modernization of the flotation machine. As it was mentioned, due to difficulties connected with modelling the flotation phenomena, only a few aspects of the process were taken under consideration. In the paper, a single phase flow of water is considered. The efficiency of the flotation process strongly depends on the fluid flow field in the machine. The level of mixing the fractions and air bubbles strongly depends on the velocity field of the water, so the proper model of fluid flow is of great practical importance. This paper presents preliminary results of mathematical modelling. The commercial package ANSYS Fluent was utilized for the analysis. The results were compared with the measurements performed on the small scale model of the machine. Obtained results are satisfying and encouraging for further development.

Keywords: flotation, multiphase flow, numerical analysis, CFD, experiments, PIV measurements.

1. INTRODUCTION

Flotation is a process commonly used in various branches of industry to separate one constituent of minerals from other ones. The flotation process of the water suspension of fine minced minerals is accomplished by the flotation machines (Fig. 1), which operation is based on differences of wettability of mineral particles. The main element of the machine is aerator (Fig. 2) consisting of a rotor and stator, which is located in a special tank. The rotor is used for mixing the water suspension of fine minced minerals (flotation pulp) as well as for dispersion of the flotation air in the pulp. The flotation air is delivered to the machine by the rotor axis. The air bubbles flowing in the pulp collide with mineral particles and create the aggregates with particles of selected minerals (hydrophobic particles attached to bubbles) called the flotation froth. The froth is lighter than water. As a result, material of lower wettability is transferred by the froth to the surface of the flotation pulp and removed by skimming device.

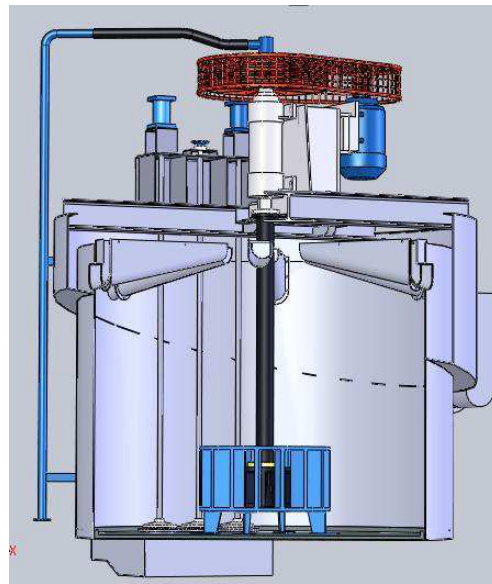


Fig. 1. Flotation machine.

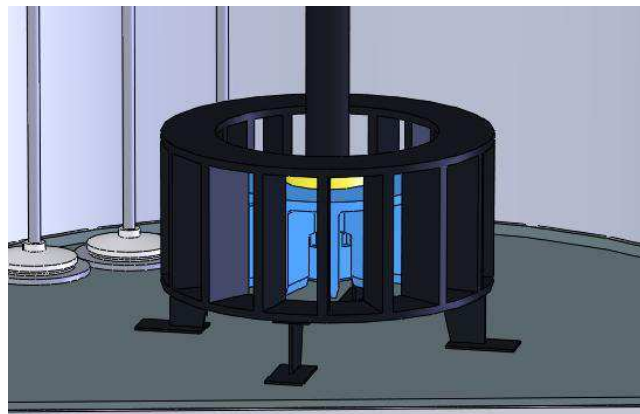


Fig. 2. Aerator of the flotation cell.

In order to improve the flotation process, a number of chemical substances are added to the flotation pulp. The additives can be distinguished with the respect to their effects as

collectors either chemically bond (chemisorption) on a hydrophobic mineral surface, or adsorb onto the surface in the case of, for example, coal flotation through physisorption. Collectors increase the natural hydrophobicity of the surface, increasing the separability of the hydrophobic and hydrophilic particles;

frothers increase the ability of the foam creation, mainly through the modification of the fluid properties, like surface tension;

modifiers improve the flotation efficiency through the modification of the physical and chemical properties of the pulp.

Complex multiphase flow phenomena take place in the flotation cells: aeration of the flotation pulp, mixing of water, air bubbles and mineral particles, creation of the flotation froth and its separation from the bulk mixture. The solid, liquid and gaseous phases interact with each other and they all participate in the flotation process. Modeling of such a process was impossible in the past. Designing the flotation machines was based on empirical formulas and experience of the designers.

Nowadays, numerical simulations of flotation phenomena became possible due to powerful enough computational machines as well as due to existence of the sophisticated computational fluid dynamic (CFD) packages to simulate flow processes, e.g., Fluent or CFX. First attempts of modeling flotation process using CFD packages can be noticed in the last decade. Results of these investigations are reported in a few papers, e.g. [2, 3, 5, 9, 10]. There are even some thematic sessions regarding modelling of the flotation phenomena (e.g., [10]) organized during conferences devoted to numerical modeling of multiphase industrial flow processes. Unfortunately, these first attempts provide rather simplified models of partial phenomena taking place during flotation. Thus, there is still a lot of problems to solve in this field. Due to mentioned complexity of phenomena, modeling of the flotation process using CFD is still a very challenging task.

The paper deals with preliminary results of modeling processes taking place in the flotation cell. At this stage, they relate to the single-phase flow of water in the flotation cell. Presented results show selected fields of velocity of the water. As it was mentioned, the structure of the water velocity field has the essential influence on the fluid and air bubbles mixing, what, on the other hand, is strongly connected with the flotation process efficiency. ANSYS Fluent CFD package was employed in the investigations. Calculations have been carried out for the small scale model of the flotation cell. Two models implemented in the ANSYS Fluent package used to simulate problems with moving domains, i.e., the so-called multiple reference frame (MRF) and “sliding mesh” have been examined. The results of the calculations have been compared to experimental observations. For this purpose the special experimental stand was built. The stand consists of the small model of the flotation machine and the PIV (particie image velocimetry) measurement system.

2. MATHEMATICAL MODEL

The fluid flow in the flotation machine experiences complex physics what is reflected in the mathematical expressions. The features of the flow are:

- three-dimensional flow,
- incompressible, Newtonian flow,
- turbulent flow,
- single-phase flow,
- unsteady state.

The phenomena in the flotation machine are described by:

- continuity equation,
- momentum equation,
- turbulence model,
- rotation model,
- spieces transport model,
- foam formation model.

At this stage of investigations only single-phase flow of water in the flotation cell is considered. Thus, the flow is simplified to a single-phase, water flow. The simplifications were undertaken to focus on the flow phenomena in the flotation machine, especially in the region surrounding the aerator. The flow field in this region affects the velocity field in the whole machine. The construction of rotor and stator significantly influences the velocity field, what makes the numerical model of

single-phase flow in the machine of great practical importance. Due to the fact, that the computations of single-phase model is much quicker than the full one, it allows to estimate the usefulness of the new constructions of aerator in the reasonable computational time.

Taking into consideration all the above simplifications, the governing equations can be presented as follows [1, 4, 7]:

- continuity equation;

$$\frac{\partial \rho u_i}{\partial x_i} = 0, \quad (1)$$

where ρ stands for the density;

- momentum equation:

$$\rho \left(\frac{du_i}{d\tau} + u_j \frac{\partial u_i}{\partial x_j} \right) = \rho g_i - \frac{\partial p}{\partial x_i} + \mu \frac{\partial^2 u_i}{\partial x_j^2}, \quad (2)$$

in the above equation, g is the gravity, p means the pressure, μ stands for the viscosity, u is the velocity vector and τ means the time;

- turbulence model.

In the paper, standard $k - \varepsilon$ model was used. For isothermal flow it can be expressed by the set of equations:

- turbulent kinetic energy k

$$\frac{\partial}{\partial \tau}(\rho k) + \frac{\partial}{\partial x_i}(\rho k u_i) = \frac{\partial}{\partial x_j} \left[\left(\mu + \frac{\mu_t}{\sigma_k} \right) \frac{\partial k}{\partial x_j} \right] + P_k - \rho \varepsilon + P_{kb}, \quad (3)$$

- dissipation ε

$$\frac{\partial}{\partial \tau}(\rho \varepsilon) + \frac{\partial}{\partial x_i}(\rho \varepsilon u_i) = \frac{\partial}{\partial x_i} \left[\left(\mu + \frac{\mu_t}{\sigma_\varepsilon} \right) \frac{\partial \varepsilon}{\partial x_i} \right] + C_{1\varepsilon} \frac{\varepsilon}{k} (P_k) - C_{2\varepsilon} \rho \frac{\varepsilon^2}{k} + C_{1\varepsilon} P_{\varepsilon b}, \quad (4)$$

where μ_t stands for the turbulent viscosity (sought for in the model):

$$\mu_t = \rho C_\mu \frac{k^2}{C_\varepsilon}, \quad (5)$$

source terms are expressed as

$$P_k = \mu_t \left(\frac{\partial u_i}{\partial x_j} + \frac{\partial u_j}{\partial x_i} \right) \frac{\partial u_i}{\partial x_j}. \quad (6)$$

The buoyancy production term P_{kb} can be expressed as

$$P_{kb} = -\frac{\mu_t}{\rho} g_i \frac{\partial \rho}{\partial x_i}. \quad (7)$$

$P_{\varepsilon b}$ represent the influence of the buoyancy forces:

$$P_{\varepsilon b} = \max(0, P_{kb}). \quad (8)$$

$C_{1\varepsilon}$, $C_{2\varepsilon}$, σ_k and σ_ε are constants [1].

The presented system of governing equations has to be completed with the well-matched pack of initial and boundary conditions. Improper selection of boundary conditions can result in enlarging the computational time, or, what is worse, in loss of convergence.

The following boundary conditions were prescribed:

- wall (no slip condition) on the walls of the tank and aerator,
- rotor: rotation 30 rad/s,
- free surface at the top of the tank.

Initial state was assumed as steady state flow with constant rotational velocity of the rotor.

3. THE EXPERIMENTAL STAND

The experimental stand was built to validate CFD models of flow processes taking place in the flotation machines. The small model of the flotation machine and the PIV [6] measurement system are the main components of the stand. This experimental stand is shown in Fig. 3. The design of the flotation cell model was adopted to requirements of the PIV technique used for the measurements of water velocity. The main parts of the cell, i.e., the container of the machine and the aerator, are made from a transparent material (plexiglas). Two kind of containers of dimensions $\phi 300 \times 600$ and $\phi 500 \times 650$ (diameter \times height, mm), can be installed in the stand, as well as two kinds of aerators, called WD and ZK. These aerators are shown in Fig. 4 and they differ in the shape of the stator blades. The rotor of the aerator is located at the bottom part of the vertical driving axle. The system is driven by an electrical engine of power 1.5 kW applied by a flexible shaft. The



Fig. 3. The experimental stand with the flotation machine.

a)

b)

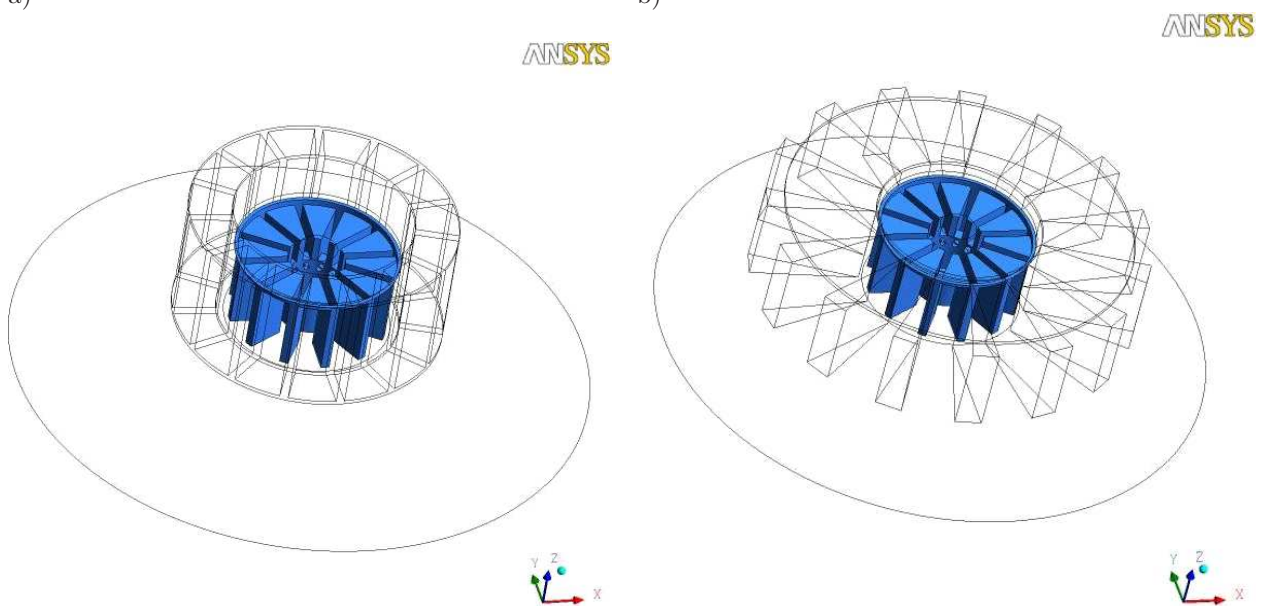


Fig. 4. a) Aerator WD and b) ZK of the flotation cell.

driving axle is also used to deliver air to the flotation cell. Speed of rotation can be changed from 100 up to 2000 rev/min. The main elements of the PIV measurement system are:

- fast digital camera Optronis CamRecord 600 with a CMOS matrix, 1024×1280 pixels,
- green constant wave diode laser of power 18 W for wavelength 532 nm,
- red back light diode illuminator of high power,
- digital camera Viewwork VC-4MC-M/C with matrix CMOSIS, 2048×2048 pixels,
- interface card Camera Link from National Instruments, PCIe-1433,
- synchronization card PCIe-6361 for devices from National Instruments,
- two-processor computer for data storage and processing.

Measured velocities have been obtained by postprocessing experimental information about the registered locations of tracer seed particles. The images postprocessing and calculations of the velocity vectors were carried out using the open toolbox written in the MATLAB environment [8]. Glass particles of diameter of order $10 \mu\text{m}$ were used as a seed. The time of averaging information was 3 s, and the thickness of illuminated measurement plane was about 3 mm. The used measurement technique does not allow to exactly determine the velocities in the domain between blades of the rotor. Errors of experimental velocities appear also in the close vicinity of the stator blades edge, because of limited transparency of these blades.

The flotation cell and measurement system are fastened to the stiff common structure.

4. NUMERICAL MODEL

ANSYS Fluent was employed for the solution of the system of equations the commercial package. Fluent utilizes control volume method to convert the governing differential equations into algebraic ones. Unfortunately, the set of governing equations is nonlinear, so the iterative procedure of solution is necessary. Additionally, the rotating elements of the aerator are the source of serious problems during the creation of numerical model. There are several possibilities of modelling rotation: mixing plane model, multiple reference frame model and sliding mesh model. All of them were taken under consideration. The distance between the rotor and stabilizer (stator) blades is shorts (about 30 mm), what is the source of transient character of phenomena taking place in the aerator. Due to that the sliding mesh model can be considered the best choice for the considered case. The rotating and stationary parts of the aerator should be separated by the so-called interface. The mesh in the rotating region slides over the stationary cells along this interface. The negative effect of such an attempt is revealed in the long term of computations. The blade transfer between the successive stator blades should be stretched to several dozen of the time steps, what with practical rotational speeds of rotor makes this time step extremely short. Therefore, also the MRF model is examined in the work, as it consumes less computational time. This is approximate, steady-state approach, also called “frozen rotor approach”, in which the mesh of rotated and stationary subdomains remains fixed during computations. As the test computations showed, the results obtained with two models: first utilizing MRF and the second with the “sliding mesh” have returned similar results. Exemplary comparisons of the results are provided in the Figs. 5 and 6. The most important conclusion is, that the simpler and faster method, MRF, can be successfully employed in the flotation machine model without the significant loss of computation quality.

Mesh generation is a significant part of CFD modeling. Although each commercial CFD package is equipped with mesh generator, this task should be performed very carefully. In fact, proper generation of mesh is one of the most time consuming parts of the whole modeling process. The quality of the mesh significantly influences the quality of the solution. Due to the lack of any symmetry,

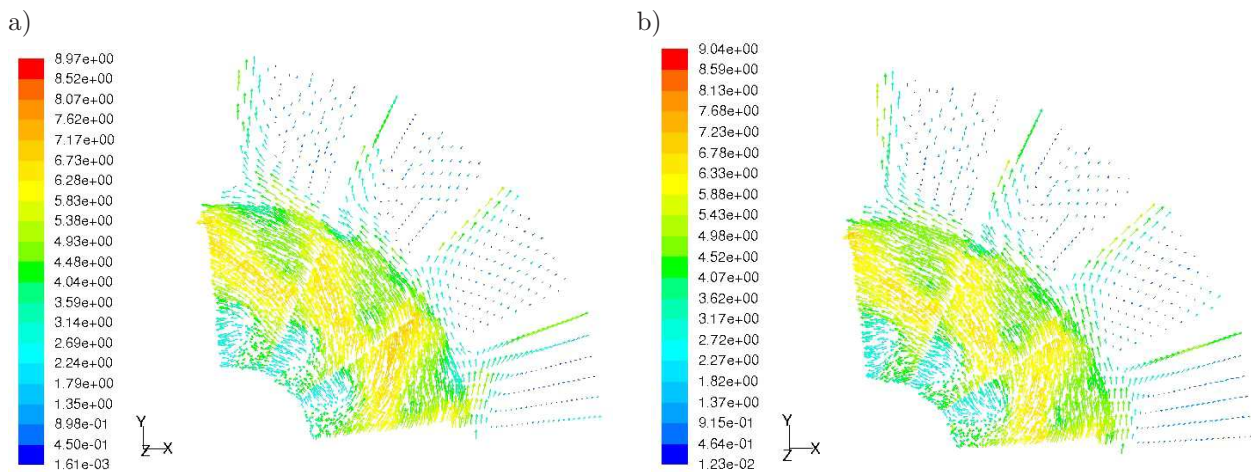


Fig. 5. Velocities on a horizontal plane for (a) MRF and (b) *sliding mesh* models, m/s, colored by velocity magnitude.

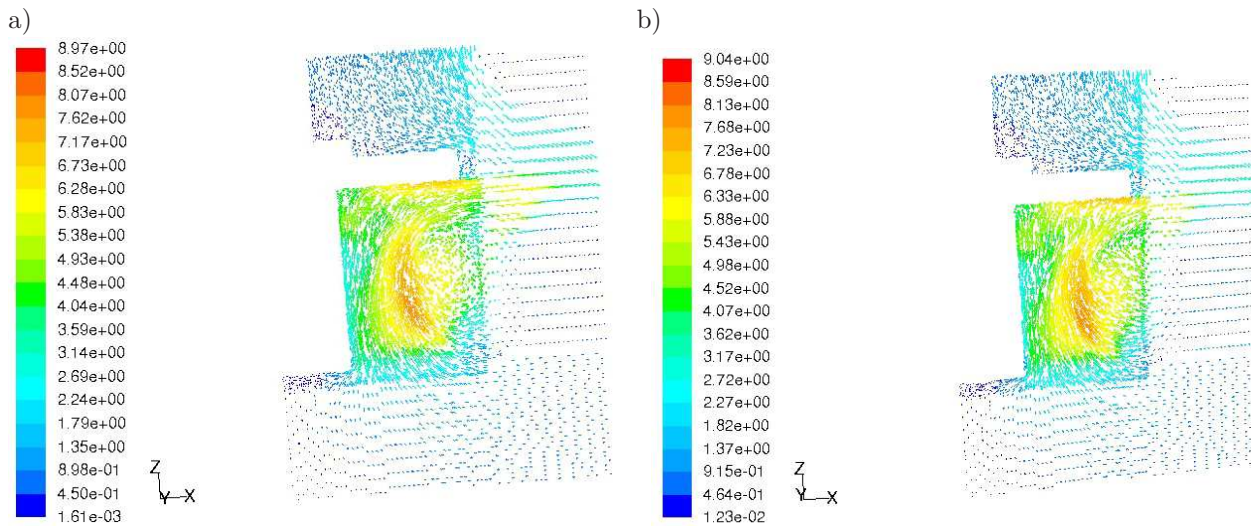


Fig. 6. Velocities on a vertical plane for (a) MRF and (b) *sliding mesh* models, m/s, colored by velocity magnitude.

the geometry of the whole machine was considered. In the presented model, the unstructured mesh was constructed with polyhedral elements. As it was mentioned previously, rotating and motionless parts of aerator were divided by an interface. The total number of elements is differed in various calculations from about 700 000 up to 4 000 000. The exemplary part of mesh is presented in Fig. 7.

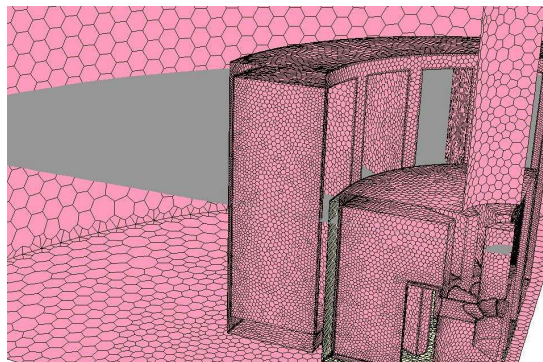


Fig. 7. Meshed aerator.

The grid independency test was performed. The velocity fields for the number of elements equal to $7E+5$ and $4E+6$ are shown in the Fig. 8. The differences between presented velocity fields are very small. Maximal values of velocities differ no more than about 3%. This means, that the grid containing about 700 000 elements can be accepted in the calculations.

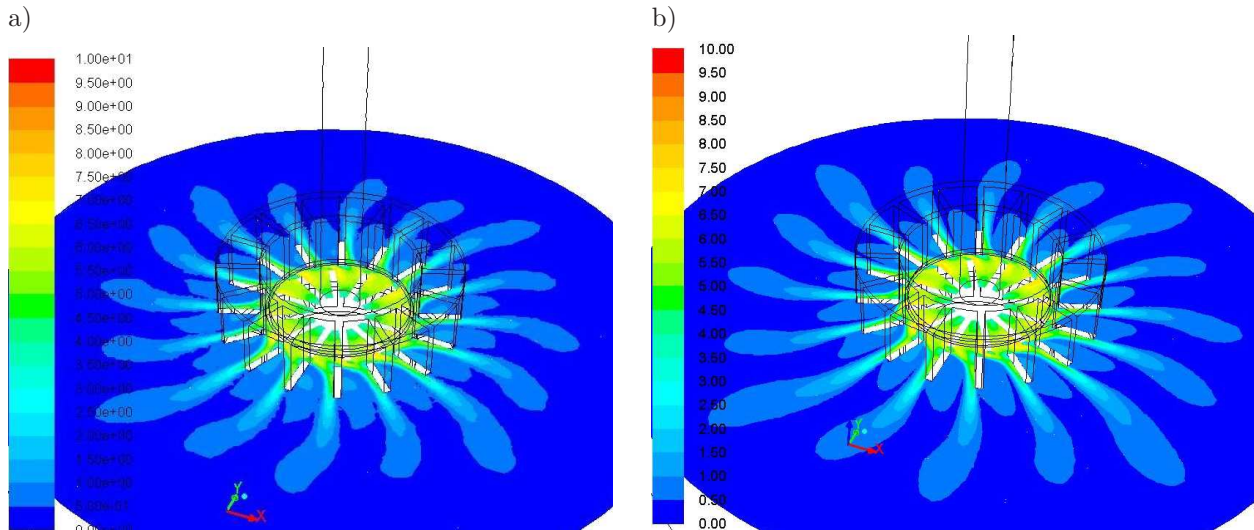


Fig. 8. Velocity distribution for (a) $7E+5$ elements and (b) $4E+6$ elements, m/s.

5. RESULTS OF COMPUTATIONS

Numerical model of the water flow within the flotation cell has been validated. The validation was based on velocity measurements by PIV performed on the experimental stand described above. Measurements and calculations have been accomplished using a tank of flotation cell of diameter equal to 500 mm and aerator of the WP type. The external radius of the rotor is 0.05 m and of the stator 0.85 m. The rotational speed of the rotor was 500 rev/min. The aerator was located at the vertical axis of the tank, and the distance from its lower edge to the bottom of the tank was 35 mm. A number of velocity measurements carried out in selected planes crossing the flotation cell have been compared with calculated velocities. Calculations were performed using the full model of the cell and the MRF technique. The mesh consisted of about 700 000 polyhedral elements. Typical properties of water were assumed.

The picture of the flotation cell, with the horizontal measurement plane located 20 mm above the container bottom (plane A), is shown in the Fig. 9. Figure 10 presents experimental compo-

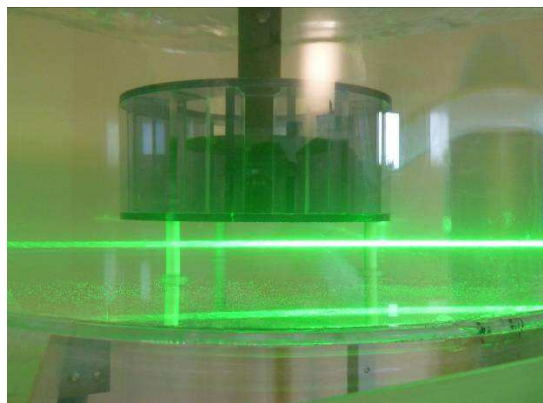


Fig. 9. The flotation cell and a horizontal measurement plane located 20 mm above the container bottom (plane A).

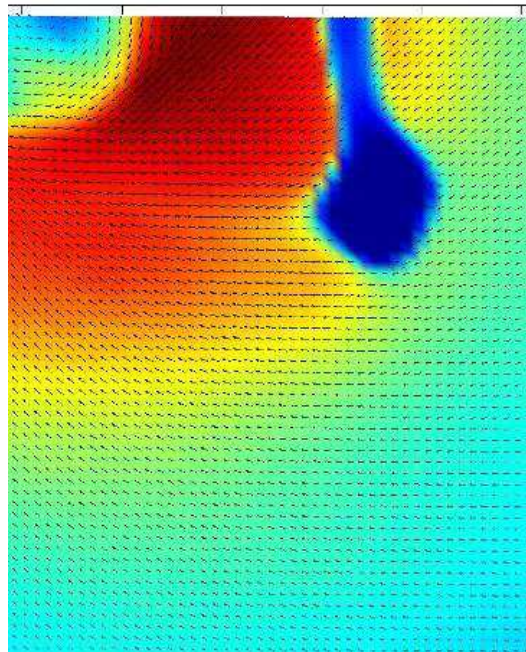


Fig. 10. Experimental velocity field components on the horizontal plane A.

nents of velocities on this plane, and Fig. 11 shows the calculated components of these velocities. The blue domain with no vectors results from a shadow of the aerator leg. Analyzed fields of measured and calculated velocity components are very similar. Water circulates in opposite direction as the rotor revolution. The same was observed experimentally. Maximal calculated value of the velocity components is 0.74 m/s, and experimental one 0.75 m/s. This difference is at the level of measurement error.

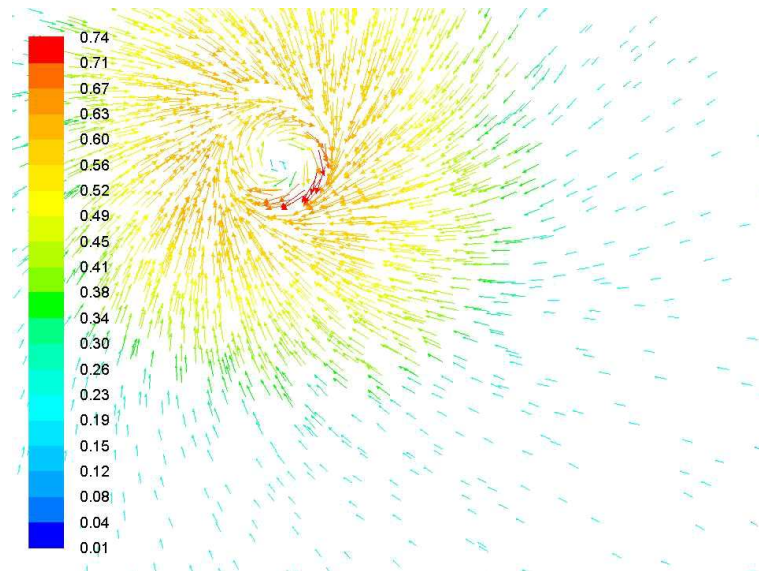


Fig. 11. Computed velocity field components on the horizontal plane A, m/s.

Figures 12 and 13 show experimental and calculated components of velocities on the horizontal plane crossing the aerator 65 mm above the tank bottom of the flotation cell (plane B) and Figs. 14 and 15 on the horizontal plane located above the aerator, 104 mm above the tank bottom (plane C).

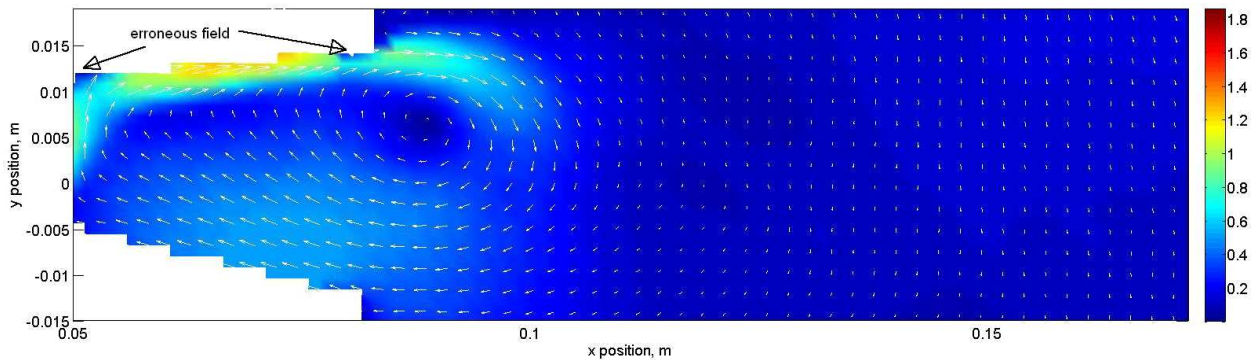


Fig. 12. Experimental velocity field components on the horizontal plane B located 65 mm above the tank bottom, m/s.

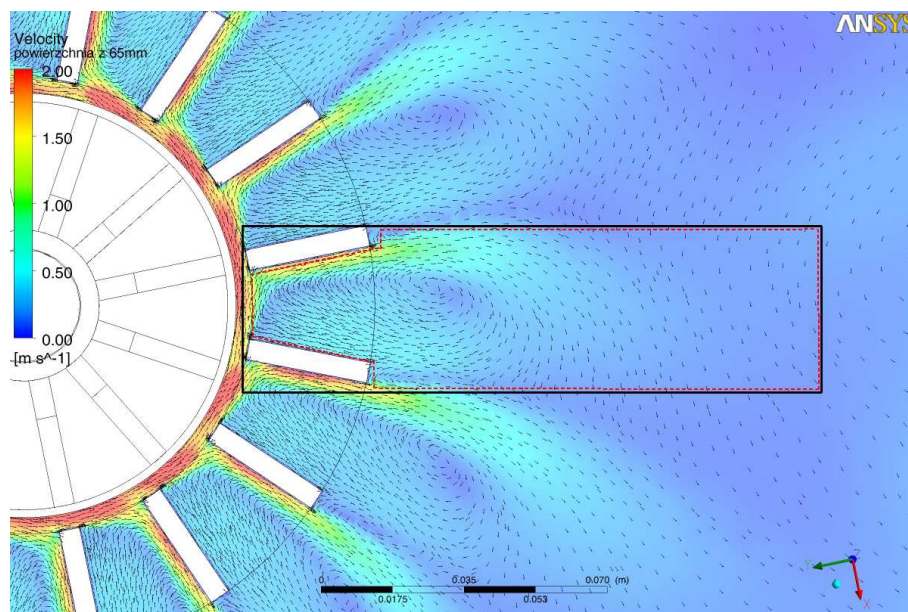


Fig. 13. Calculated velocity field components on the horizontal plane B located 65 mm above the tank bottom with marked measurement domain from Fig. 12.

The centre of the driving axle is located at point $x = 0$ in Figs. 12 and 14. Figure 12 presents experimental components of velocities in the segment of the domain containing a space between two successive blades of stator and in a part of the domain outside the aerator, while Fig. 14 only outside of the aerator. These segments of the domain are marked in Figs. 13 and 15, respectively.

The structure of the experimental and calculated velocity fields on the plane B shown in Figs. 12 and 13 is very similar. Some errors in experimental velocities can be observed in immediate vicinity of the stator blades edges (blue spots along their surfaces where high values of velocity are expected). This is the result of mentioned limited transparency of the stator blades. It is worth noting that simulations allow to correctly predict the eddies outside the stator blades. Maximum values of measured and calculated velocity components within the analyzed domain are also very close (about 2 m/s). The structure of the experimental and calculated velocity fields on the plane C shown in Figs. 14 and 15 is also very similar, and maximum values of the velocity components obtained are very close (about 1.3–1.4 m/s).

One can conclude, that the used model of the water flow in the flotation cell and applied technique of solving the problem allow to predict the velocity field in the cell with satisfying accuracy. Large differences between the measured and calculated velocities were observed within relatively small domain in the vicinity of the interface between the rotor and the stator. This is the result of both

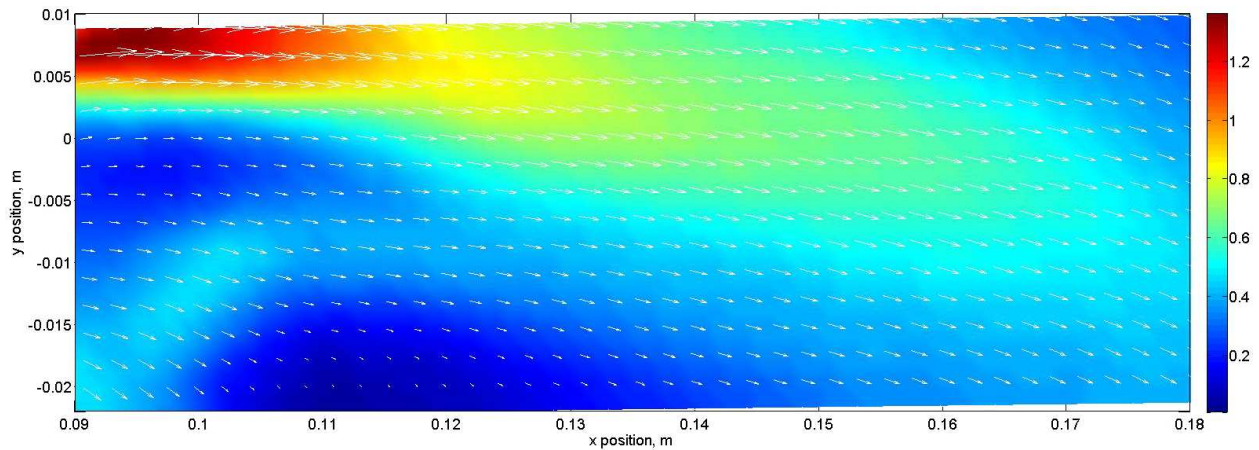


Fig. 14. Experimental velocity field components on the horizontal plane C located 104 mm above the tank bottom, m/s.

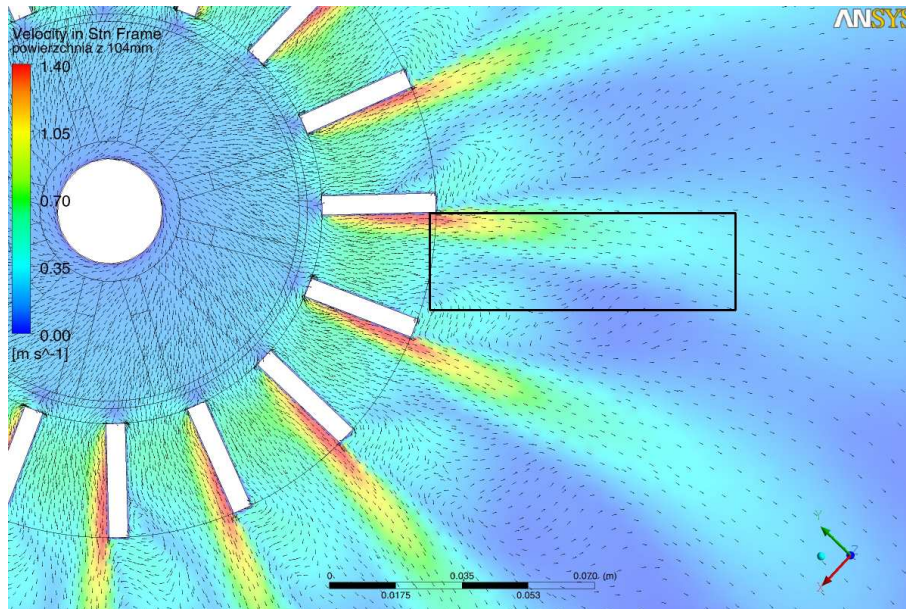


Fig. 15. Calculated velocity field components on the horizontal plane C located 104 mm above the tank bottom with marked measurement domain from Fig. 14.

measuring and computational errors. To overcome the errors the sliding mesh technique has to be used, which is impossible in this context as it requires solving a time-dependent problem with a very short time step and such calculations consume a lot of computational time. Experimentally determined velocities between the rotor blades are completely useful due to measuring errors. Measurements do not also allow to achieve exact values of velocities in the immediate vicinity of the stator blade edges.

6. CONCLUSIONS AND FUTURE WORK

The model of water flow in the flotation cell prepared in the ANSYS Fluent package is presented in this paper. The model was tested and validated against the PIV velocity measurements performed on a special experimental stand. For this purpose, a number of numerical tests were carried out using various grids, MRF and sliding mesh techniques to resolve rotor revolution. The tests show that the grid containing about 700 000 polyhedral elements in the full model of the experimental cell

is enough from the accuracy point of view. The usage of the MRF technique is a good compromise, as the sliding mesh requires time-dependent calculations with a very short time step and they consume a lot of computational time. Comparison of experimental and numerical velocity fields show a satisfactory agreement in the most important part of the considered domain from the flotation process point of view, i.e., outside of the aerator. The structure of analysed fields, as well as values of velocities, are generally similar in analysed domain. However, this can be explained by known experimental and numerical errors and can be accepted, as it concerns relatively small region of the flotation machine.

The future work anticipates application of the prepared model to analyze mixture processes of water in different flotation cells with various types of aerators, various speeds of the rotor revolution. Extension of the model on multiphase flows in the flotation machines containing flotation air and flotation materials is also planned.

ACKNOWLEDGEMENTS

The financial support of The National Centre for Research and Development, Poland, within the grant NR02 0102-10/2010 is gratefully acknowledged herewith.

REFERENCES

- [1] ANSYS Fluent 12.1.4. Theory Guide, April 2009.
- [2] D.A. Deglon, C.J. Meyer. CFD modelling of stirred tanks: Numerical considerations. *Minerals Engineering*, **19**: 1059–1068, 2006.
- [3] A. Fic, A. Sachajdak, I. Szczygieł, A. Mańka. *Flow processes in the aerator of the flotation machine preliminary simulations*. XX Jubileuszowy Zjazd Termodynamików 2008. Termodynamika w Nauce i Gospodarce, Z. Gnutek, W. Gajewski [Eds.], Vol. I, 260–267, Oficyna Wydawnicza Politechniki Wrocławskiej, Wrocław, 2008 (in Polish).
- [4] M. Ishii, T. Hibiki. *Thermo-Fluid Dynamics of Two-Phase Flow*. Springer, New York, 2010.
- [5] P.T.L. Koh, M.P. Schwarz. CFD model of self-aerating flotation cell. *Int. J. Mineral Process*, **85**: 16–24, 2007.
- [6] M. Raffel, C. Willert, S. Wereley, J. Kompenhans. *Particle image velocimetry. A practical guide*. Springer-Verlag, 2nd edition, Berlin, 2007.
- [7] D. Ramkrishna. *Population Balances: Theory and Applications to Particulate Systems in Engineering*. Academic Press, 2000.
- [8] J.K. Sveen, E.A. Cowen. *Quantitative imaging techniques and their application to wavy flow*. In J. Grue, P.L.F. Liu, G.K. Pedersen [Eds.], *PIV and Water Waves*. World Scientific, 2004.
- [9] I. Szczygieł, A. Fic, A. Sachajdak, M. Rojczyk, Z. Bulinski. *Numerical analysis of the water aeration in the flotation machine*. Proc. of 10th World Congress on Computational Mechanics, Sao Paulo, Brasil, 2012.
- [10] J. Tiitinen, J. Vaarno, S. Grnstrand. *Numerical modelling of an Outokumpu flotation device*. 3th Int. Conf. on CFD in the Minerals and Process Industries, Melbourne, Australia, 2003.